

Theory of Use of Granulated Materials in Road Construction

VALERY A. SEMENOV

The use of granulated materials (especially low-strength materials) in pavements is limited because such materials undergo significant breakage during packing and use. The breakage is mainly due to the extraordinary contact stresses in the particles of the material, which lead to its fragmentation and the formation of melkozem (fine earth) and a sharp decrease in the strength of the material. The method presented here for calculating and controlling the contact stresses in granulated material is the first attempt at the theoretical calculation of stresses in a stochastic medium. Using the model for the stochastic packing of granulated materials proposed by the author as a starting point, the packing density, the number of contacts in an arbitrary cross section through the material, the area of contact between individual particles, and the contact stresses are calculated. The theory presented in this paper makes it possible to carry out various theoretical calculations associated with engineering process control and monitoring of the strength of material over the service life of a road covering, and it can also be used for other problems.

Local low-strength materials and industrial by-products are used for highway construction in many countries. The strength of these materials averages from 30 to 40 MPa, so they undergo fragmentation in packing and a large number of fine particles (up to 22 percent) are formed. The process of particle fragmentation continues over the lifetime of the road. This lowers the usable lifetime of the pavement to from 5 to 7 years. Stronger materials (with a strength of from 80 to 140 MPa) are similarly damaged, but this process proceeds more slowly.

Particle fragmentation is due to the high contact stresses that arise in the material; reducing these stresses during the packing process and under exposure to traffic will allow low-strength materials to be used and their life span in road coverings to be increased. There are currently no methods of calculating the contact stresses in complex stochastic media (any real granulated material, such as crushed stone, gravel, sand, soil).

The purpose of this paper is to develop a theoretical model and engineering methods for calculating stresses in granulated materials. A stochastic model and theoretical nomograms have been developed for calculating contact stresses. The proposed model includes the packing of particles of various sizes and shapes. The results presented here are based on 5 years of research carried out by the author at the Vladimir Polytechnical Institute (Vladimir, USSR).

Department of Civil Engineering, The University of Texas at Austin, Austin, Tex. 78712. Permanent affiliation: School of Highway and Agricultural Construction and Highway Department, The Polytechnical Institute of Vladimir Gorky, 87, Vladimir, 600 005 USSR.

THEORETICAL MODEL FOR DETERMINING THE PACKING DENSITY OF A STOCHASTIC MEDIUM

Packing density may be determined from geometric considerations by averaging the results of a large number of iterations with respect to random packings composed of individual particles. The number of iterations is determined by the required accuracy of calculation and ranges from 100 to 300.

The particle sizes in each iteration are selected randomly (using the Monte Carlo method, the Korobov algorithm, or a table of random numbers). The continuous-sorting method may also be used. The volume packing density (ρ) is defined as

$$\rho = \frac{v_{\text{avg}}}{V_{\text{avg}}} = \frac{\int_D v(r) f(r) dr}{\int_D V(r) f(r) dr} \quad (1)$$

where

- v = the volume occupied by the particles of the material in an arbitrary tetrahedron,
- V = the volume of the tetrahedron,
- $f(r)$ = the particle size distribution function,
- D = the region in space ($r_{\min} \leq r \leq r_{\max}$, $r > 0$), and
- r_{\min} and r_{\max} = the minimum and maximum sizes of the particles of material in the packing.

This formula may be used as long as the following condition is satisfied:

$$\frac{r_1}{r_4} \leq 1 + \frac{r_1}{r_2} + \frac{r_1}{r_3} + 2 \sqrt{\frac{r_1}{r_2} + \frac{r_1}{r_3} + \frac{r_1 r_1}{r_2 r_3}} \quad (2)$$

where r_1 , r_2 , r_3 , and r_4 are the radii of the particles in the packing in a given iteration and r_4 is the minimum radius. An analysis of Equation 2 showed that the proposed model can be used for any highway construction materials or soils. The volume density (ρ_{in}) is determined by using Equation 1 to average the results of the determination of the density of a packing consisting of four random radii at each iteration. The calculation procedure presented hereafter is used to determine

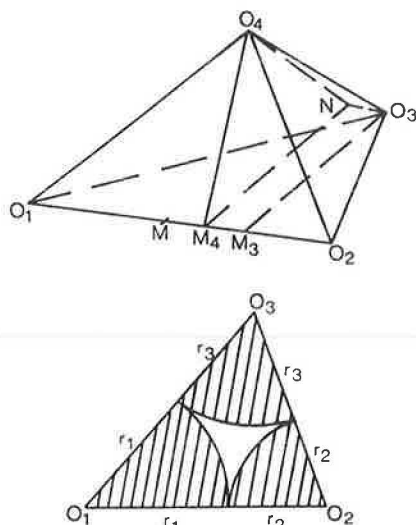


FIGURE 1 Theoretical diagram of stochastic packing.

the packing density at each iteration. Figure 1 is a diagram that shows the determination of r_{in} (where O_1 , O_2 , O_3 , and O_4 are the centers of the particles that are in contact).

The value of $O_3M_3 = h_3$ from the triangle $O_1O_2O_3$ is determined by using Heron's formula:

$$S_{O_1O_2O_3} = \sqrt{r_1 r_2 r_3 (r_1 + r_2 + r_3)}$$

At the same time,

$$S_{O_1O_2O_3} = \frac{1}{2}(r_1 + r_2)h_3$$

Equating these two expressions gives

$$h_3 = \frac{2\sqrt{r_1 r_2 r_3 (r_1 + r_2 + r_3)}}{r_1 + r_2} \quad (3)$$

To determine $|M_3M_4|$, the geometric center of the edge O_1O_2 is denoted by M ; then

$$|M_3M_4| = |X_3 - X_4| \quad (4)$$

where $X_3 = MM_3$ is the distance between the foot of altitude h_3 and Point M , and $X_4 = MM_4$ is the distance from the foot of altitude h_4 to Point M . The value of X_3 can be determined from triangle $O_1O_2O_3$ using the Pythagorean theorem:

$$(r_1 + r_3)^2 - h_3^2 = \left(\frac{r_1 + r_2}{2} + X_3\right)^2$$

and

$$(r_2 + r_3)^2 - h_3^2 = \left(\frac{r_1 + r_2}{2} + X_3\right)^2$$

from which, after a system of two equations is solved, is obtained

$$X_3 = \frac{r_1 - r_2}{r_1 + r_2} \left(\frac{r_1 + r_2}{2} + r_3 \right)$$

Similarly, the value of X_4 can be obtained from the triangle $O_1O_2O_4$, and

$$|M_3M_4| = \left| \frac{(r_1 - r_2)(r_3 - r_4)}{r_1 + r_2} \right|$$

can be determined using Equation 4. By the Pythagorean theorem, $|NO_4| = h_0$ can be obtained from the triangle O_3NO_4 :

$$h_0 = \frac{1}{r_1 + r_2} \sqrt{(r_1 + r_2)^2 (r_3 + r_4)^2 - (r_1 - r_2)^2 (r_3 - r_4)^2}$$

By the cosine theorem, from the triangle M_4O_4N is obtained

$$h_0^2 = h_3^2 + h_4^2 - 2h_3h_4 \cos \gamma_{12} \quad (5)$$

where γ_{12} is the dihedral angle with the edge O_1O_2 . Using Equation 5, it is found that

$$\cos \gamma_{12} = \frac{h_3^2 + h_4^2 - h_0^2}{2h_3h_4}$$

The volume of the tetrahedron $O_1O_2O_3O_4$ can now be determined:

$$V = \frac{1}{6} h_3 h_4 \sin \gamma_{12} (r_1 + r_2) \quad (6)$$

From Equation 6, it follows that

$$\sin \gamma_{12} = \frac{1}{2h_3h_4} \sqrt{4h_3^2h_4^2 - (h_3^2 + h_4^2 - h_0^2)^2}$$

Hence,

$$V = \frac{1}{12} (r_1 + r_2) \sqrt{4h_3^2h_4^2 - (h_3^2 + h_4^2 - h_0^2)^2} \quad (7)$$

From Expression 3,

$$h_3h_4 = \frac{4}{(r_1 + r_2)^2} \left[r_1r_2(r_1 + r_2)(r_3 + r_4) - r_3r_4(r_1^2 + r_2^2) \right] \quad (8)$$

The following notation is now introduced:

$$\begin{aligned} \sigma_1 &= r_1 + r_2 + r_3 + r_4 \\ \sigma_2 &= r_1r_2 + r_1r_3 + r_1r_4 + r_2r_3 + r_2r_4 + r_3r_4 \\ \sigma_3 &= r_1r_2r_3 + r_1r_2r_4 + r_1r_3r_4 + r_2r_3r_4 \\ \sigma_4 &= r_1r_2r_3r_4 \\ a &= r_1 + r_2 \\ A &= r_1r_2 \\ b &= r_3 + r_4 \\ B &= r_3r_4 \end{aligned} \quad (9)$$

Then,

$$h_3 h_4 = \frac{4}{a^2} \sqrt{A^2 B (a^2 + ab + B)}$$

$$h_3^2 + h_4^2 - h_0^2 = \frac{4}{a^2} (abA - a^2 B + 2AB) \quad (10)$$

Substituting Equation 10 into Equation 7,

$$V = \frac{1}{3} \sqrt{4\sigma_2 \sigma_4 - \sigma_3^2} \quad (11)$$

The volume (v) occupied by the spherical segments within the tetrahedron with centers at the Points O_i (Figure 1) can now be determined. Suppose that there is a spherical triangle ($M_1 M_2 M_3$) on a sphere of radius R (i.e., the arcs $M_1 M_2$, $M_2 M_3$, and $M_1 M_3$ are segments of great circles). The angles formed by the tangents to the arcs will be designated by γ_1 , γ_2 , and γ_3 (Figure 2).

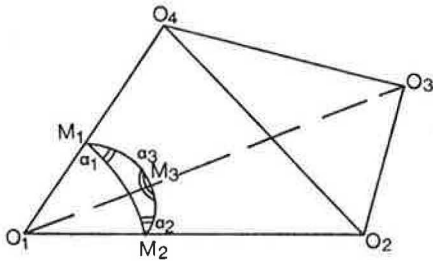


FIGURE 2 Diagram for determining the volume of solids within the tetrahedron.

By Gauss's theorem,

$$S_{M_1 M_2 M_3} = R^2 (\gamma_1 + \gamma_2 + \gamma_3 - \pi)$$

Hence,

$$v_{O_1 M_1 M_2 M_3} = \frac{R^3}{3} (\gamma_1 + \gamma_2 + \gamma_3 - \pi)$$

Note that the angle $M_1 M_2 M_3 = \gamma_2 = \gamma_{12}$, and so forth. Then

$$v = \sum_{i < j} \frac{1}{3} (r_i^3 + r_j^3) \gamma_{ij} - \frac{p}{3} \sum_{i=1}^4 r_i^3 \quad (12)$$

($i, j=1, 2, 3, 4$)

The dihedral angles γ_{ij} may be determined by transforming Equation 6 using the notation of Equation 9 and Equations 10:

$$\cos \gamma_{ij} = \frac{r_i r_j \sigma_2 - (r_i r_j)^2 - \frac{r_i + r_j}{2} \sigma_3}{\sqrt{r_i r_j (r_i + r_j) \sigma_1 \sigma_4 + \sigma_4^2}} \quad (13)$$

Equation 13 may be used to obtain all six values of the angles.

The stochastic model that has been developed for the dense packing of particles of soil and other materials can be used extensively in highway construction and maintenance. Thus it is possible to calculate the theoretical density of asphalt con-

crete, cement concrete, crushed stone, gravel, and soil. This makes it possible to substantially improve density norms and develop an optimal production technology. It is also possible to use this model to calculate the contact stresses in particles of material, for which it is necessary to determine the individual contact area between the particles in the material and the total number of contacts in a random cross section.

DETERMINATION OF THE AREA OF CONTACT BETWEEN PARTICLES IN THE MATERIAL

In determining the area of contact, it is assumed that the particle size distribution is known, and the particles will be represented by two concentric spheres with radii R_0 and R_1 given by the minimum and maximum particle radii (Figure 3). It is assumed that there is some probability $[p(x)]$ for material to be found within a sphere of radius R_1 ; this probability is equal to 1 for a sphere with radius R_0 . Probability $p(x)$ is obtained from experimental data. It is also assumed that some interpenetration of spheres is possible, and the amount of interpenetration is denoted by α (Figure 3).

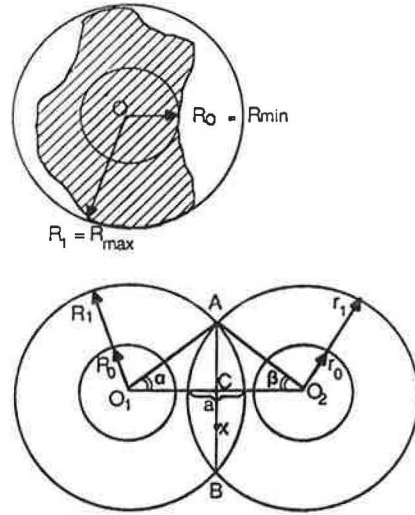


FIGURE 3 Diagram for determining the area of contact between particles.

To determine the area of contact, it will be assumed that the area is equal to the area formed by rotating line AB about Point C :

$$S_{AB} = 2\pi \int_0^{R_1 \sin \alpha} t p_1 \left(\sqrt{t^2 + R_1^2 \cos^2 \alpha} \right) dt$$

$$x = \sqrt{t^2 + R_1^2 \cos^2 \alpha} \quad (14)$$

Then,

$$S_{AB} = 2\pi \int_{R_1 \cos \alpha}^{R_1} x p_1(x) dx$$

If two particles of different sizes participate in the contact, the area of contact will be given by the arithmetic mean of the areas of contact for each particle:

$$S_a = \frac{S_{AB} + S_{BA}}{2} = \pi \left[\int_{R_1 \cos \alpha}^{R_1} x p_1(x) dx + \int_{r_1 \cos \beta}^{r_1} x p_2(x) dx \right] \quad (15)$$

The parameters A , B , and a must be expressed in probabilistic form. To do this, the contact between the particles is represented by graphs of the probabilities $p_1(x)$ and $p_2(x)$ (Figure 4).

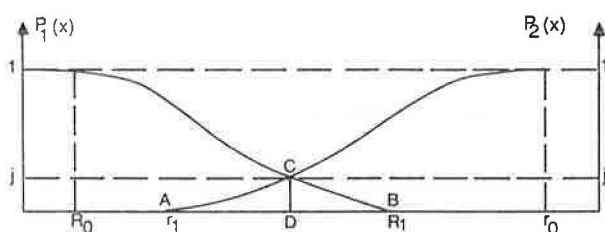


FIGURE 4 Diagram for calculating the depth of interpenetration for the spheres used to model the particles of material.

It is assumed that the parameter describing the depth to which the spheres penetrate one another is $CD = j$. From Figure 4,

$$AD = r_1 - t'_{1-j} \text{ and } BD = R_1 - t_{1-j}$$

where t_{1-j} and t'_{1-j} are the $(1-j)$ th quantiles. It is now found that $a = r_1 + R_1 - (t_{1-j} + t'_{1-j})$, so that Equation 15 takes the following form:

$$S_j = \pi \left[\int_{t_{1-j}}^{R_1} x p_1(x) dx + \int_{t'_{1-j}}^{r_1} x p_2(x) dx \right] \quad (16)$$

Rewriting Equation 16,

$$\begin{aligned} \int_{t_{1-j}}^{R_1} x p_1(x) dx &= \int_{t_{1-j}}^{R_1} x [1 - F_1(x)] dx \\ &= \frac{x^2}{2} \Big|_{t_{1-j}}^{R_1} - \int_{t_{1-j}}^{R_1} x \left[\int_{-\infty}^x f(t) dt \right] dx \\ &= \frac{1}{2} (R_1^2 - t_{1-j}^2) - \int_{(0)}^{t_{1-j}} x f(t) dt dx \\ &= \frac{1}{2} (R_1^2 - t_{1-j}^2) - \int_{-\infty}^{t_{1-j}} \left(\frac{x^2}{2} \Big|_{t_{1-j}}^{R_1} \right) f(t) dt \end{aligned}$$

$$\begin{aligned} &= - \int_{t_{1-j}}^{R_1} \left(\frac{x^2}{2} \Big|_{t_{1-j}}^{R_1} \right) f(t) dt \\ &= - \frac{\gamma t_{1-j}^2}{2} + \frac{1}{2} \int_{t_{1-j}}^{R_1} t^2 f(t) dt \end{aligned}$$

it is found that

$$S_j = \frac{\pi}{2} \left[\int_{t_{1-j}}^{R_1} t^2 f_1(t) dt + \int_{t'_{1-j}}^{r_1} t^2 f_2(t) dt - j(t_{1-j}^2 + t'_{1-j}^2) \right] \quad (17)$$

Equation 17 is a general expression for determining the contact area between particles. Several specific examples will be discussed next.

Example 1

When both particles have a uniform distribution of radii (Figure 5), it is found that

$$t_{1-j} = R_0 + (1-j)(R_1 - R_0) = R_1 - j(R_1 - R_0)$$

Then,

$$S_j = \frac{j^2 \pi}{3} (R_1 - R_0) [3R_1 - 2j(R_1 - R_0)] \quad (18)$$

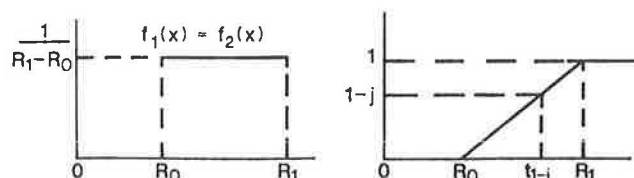


FIGURE 5 Diagram for Example 1.

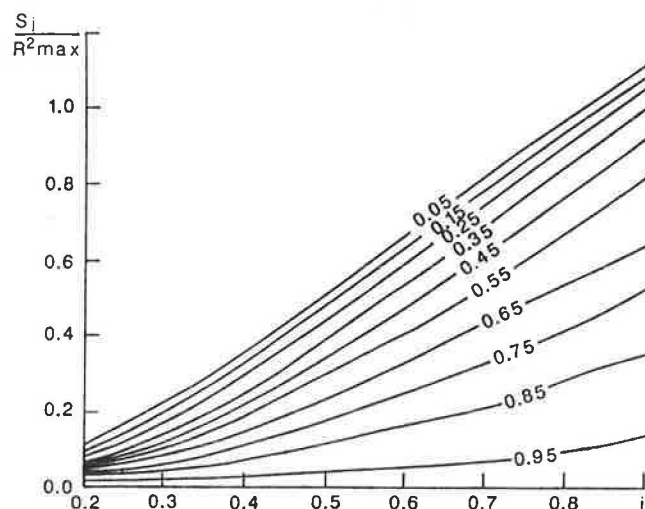


FIGURE 6 Nomogram for determining the areas of contact between particles with a normal distribution of radii.

Equation 18 was then used to construct a nomogram (Figure 6). Suppose that $R_1 = 2$ cm, $R_0 = 1$ cm, and $j = 0.5$; then,

$$S_j = \frac{3.14}{4 \cdot 3} (2.1) [3 \cdot 2 - 2 \cdot 0.5(2 - 1)] = 1.3 \text{ cm}^2$$

The surface area of the larger sphere is

$$S_1 = 4\pi R_1^2 = 50.2 \text{ cm}^2$$

Thus, the relative area of contact is

$$S_{\text{rel}} = \frac{1.3 \cdot 100}{50.2} = 2.7 \text{ percent}$$

Example 2

For the case of normally distributed particle radii, the following expressions are obtained:

$$S'_j = \pi \left((0.5 - jt_{1-j}^2) \sigma^2 + \frac{2\sigma m}{(2\pi)^{1/2}} \left\{ \left[\exp \left(-t_{1-j}^2 / 2 \right) \right] - t_{1-j} (2\pi)^{1/2} \right\} - Ft_{1-j} \right) \quad (19)$$

$$S'_j = \frac{S'_j + S''_j}{2} \quad (20)$$

where

- S'_j and S''_j = the areas of contact for the first and second particles, respectively;
- m = the mathematical expectation value of the particle radius;
- s = the root-mean-square deviation of the particle radii; and

$$Ft_{1-j} = \frac{1}{(2\pi)^{1/2}} \int_0^{t_{1-j}} t^2 \exp(-t^2/2) dt$$

The quantile t_{1-j} can now be determined by using the following equation:

$$\frac{1}{2} - j = \Phi \left(\frac{x_{1-j} - m}{\sigma} \right) \quad (21)$$

where

$$\Phi \left(\frac{x_{1-j} - m}{\sigma} \right)$$

is the Laplace function. For $j = 0.5$, the quantile $x_{(j=0.5)} = r_{\text{avg}}$, and the equation becomes much simpler:

$$S_{0.5} = \pi \sigma \left[\frac{\sigma}{2} + \left(\frac{2}{\pi} \right)^{1/2} r_{\text{avg}} \right] \quad (22)$$

A nomogram has been constructed from Equation 22 (Figure 7). Suppose that $r_{\text{avg}} = 2$ cm, and $s = 0.2$ cm. Then

$$S_{0.5} = 3.14 \cdot 0.2 \left(\frac{0.2}{2} + 0.8 \cdot 2 \right) = 1.07 \text{ cm}^2$$

which is about 2 percent of the surface area of the larger sphere.

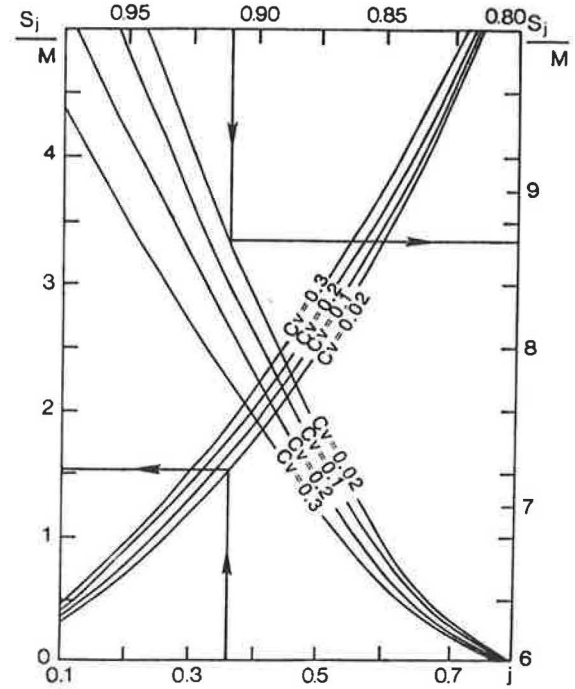


FIGURE 7 Nomogram for determining the particle contact area when the particle radii are normally distributed.

Example 3

For the Weibull distribution of particle radii Weibull's law may be written in the form

$$f(x) = \lambda k (x - r_{\min})^{k-1} \exp[-\lambda(x - r_{\min})^k] \quad (23)$$

where λ and k are the scale and form parameters, respectively. The quantile x_{1-j} may be calculated from the equations

$$j = e^{-\lambda(x_{1-j} - r_{\min})^k} \quad (24)$$

$$x_{1-j} = r + \left(\frac{1}{\lambda} \ln \frac{1}{j} \right)^{1/k}$$

By substituting Equation 23 into Equation 17 and rearranging, it is found that

$$S'_j = \pi \left(\frac{1}{\lambda} \right)^{2/k} \bar{A}_1 + 2\pi r_{\min} \left(\frac{1}{\lambda} \right)^{1/k} \bar{A}_2 \quad (25)$$

Rearranging Equation 25,

$$S'_j = (r_{\text{avg}} - r_{\min})^2 A_1 + r_{\min} (r_{\text{avg}} - r_{\min}) A_2 \quad (26)$$

where

$$A_1 = \frac{\pi}{\Gamma\left(1 + \frac{1}{k}\right)^2} \bar{A}_1$$

$$A_2 = \frac{2\pi}{\Gamma\left(1 + \frac{1}{k}\right)} \bar{A}_2$$

$$\bar{A}_1 = \Gamma\left(1 + \frac{2}{k}\right) - j\left(\ln \frac{1}{j}\right)^{2/k} - \int_0^{\ln 1/j} t^{2/k} \exp(-t) dt$$

$$\bar{A}_2 = \Gamma\left(1 + \frac{1}{k}\right) - j\left(\ln \frac{1}{j}\right)^{1/k} - \int_0^{\ln 1/j} t^{1/k} \exp(-t) dt$$

and $\Gamma(z)$ is the gamma function.

The final value of the area of contact is given by Equation 20. A nomogram (Figure 8) was constructed using these equations.

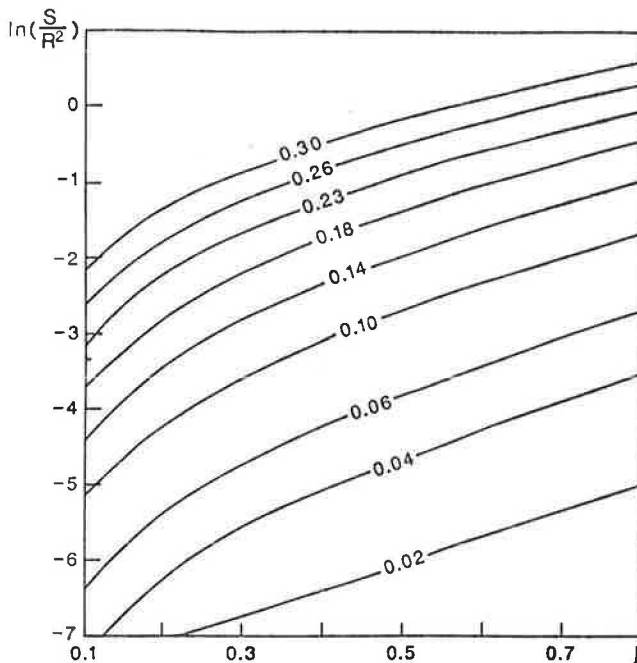


FIGURE 8 Nomogram for calculating the area of contact between particles that have a Weibull distribution with variable parameters.

Suppose that

$$\begin{aligned} R_{\text{avg}} &= 2 \text{ cm, } CV_R = 0.10: j = 0.5; \text{ therefore, } S_j = 0.26 \text{ cm}^2 \\ R_{\text{avg}} &= 2 \text{ cm, } CV_R = 0.04: j = 0.5; \quad S_j = 0.04 \text{ cm}^2 \\ R_{\text{avg}} &= 2 \text{ cm, } CV_R = 0.10: j = 0.3; \text{ therefore, } S_j = 0.10 \text{ cm}^2 \\ R_{\text{avg}} &= 1 \text{ cm, } CV_R = 0.10: j = 0.5; \quad S_j = 0.064 \text{ cm}^2 \end{aligned}$$

where CV_R is the coefficient of variation of the particle radii.

Thus, the area of contact increases with increasing j , D , and R_{avg} .

This solution has been thoroughly tested by N. M. Egorov, an engineer at the Vladimir Polytechnical Institute. The value of j for individual particles of crushed stone varied over a wide range from 0.071 to 1.000 with an average value of $j = 0.5$. The contact area between the particles ranged from 3 to 707 mm^2 . A comparison of the theoretical and experimental values of the contact area showed that the difference between them is no greater than 12 percent, so that the solution obtained may be used extensively in practical calculations.

DETERMINATION OF THE NUMBER OF CONTACTS BETWEEN PARTICLES OF MATERIAL IN A RANDOM CROSS SECTION

To determine contact stresses, an expression must be obtained for the number of contacts in an arbitrary plane passing through some volume of granulated material. Imagine that there is a connection between the particles in the form of the edge of a graph (a line connecting the centers of the particles). The probability that this edge (AB) is intersected by an arbitrary plane (Figure 9) is to be determined. The position of the edge in space may be characterized by three numbers: (a) the length of the edge (l), (b) the distance from the center of the edge to the intersecting plane (x), and (c) the angle between the edge and

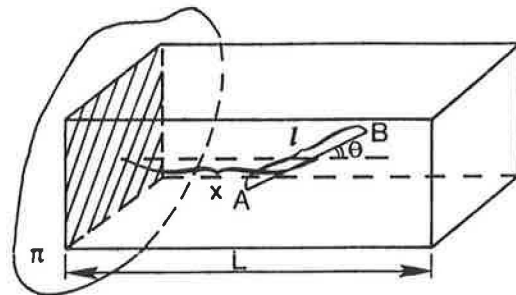


FIGURE 9 Theoretical diagram for determining the number of contacts between particles in a plane passing through the packing.

the horizontal (θ). These are all random quantities with corresponding probability density functions $p(l)$, $p(x)$, and $p(\theta)$. The limits of variation for l , θ , and x are $l_{\min} \leq l \leq l_{\max}$, $0 \leq \theta \leq \pi/2$, and $0 \leq x \leq L$. It is assumed that the quantity x is uniformly distributed, so that

$$p(x) = \begin{cases} 1/L & x \in [0, L] \\ 0 & x \notin [0, L] \end{cases} \quad (27)$$

The edge is intersected by the plane (p) if and only if $x < (l/2) \cos \theta$. The probability that the edges intersect the plane p will be designated. Then,

$$p = \int \int \int_{(V)} p(l)p(\theta)p(x) dl d\theta dx$$

$$\begin{aligned}
&= \int_0^{\pi/2} d\theta \int_{l_{\min}}^{l_{\max}} \frac{1}{2} \cos \theta p(l) p(\theta) dl \\
&= \frac{l_{\text{avg}}}{2L} \int_0^{\pi/2} \cos \theta p(\theta) d\theta
\end{aligned} \quad (28)$$

where V is the volume of the material.

The number of particles within the volume $[V(N_p)]$ may be obtained from the following equations:

$$\begin{aligned}
LS\rho &= \frac{4\pi}{3} r_{\text{avg}}^3 N_p \\
N_p &= \frac{3LS\rho}{4\pi r_{\text{avg}}^3}
\end{aligned} \quad (29)$$

where

- L and S = the dimensions of the volume being studied (see Figure 9),
 r = the volume packing density of the material, and
 r_{avg} = the mean particle radius in the packing of the material.

The number of contacts between particles in a volume $[V(N_p)]$ is

$$Q_r = \frac{1}{2} k N_p = \frac{3kL\rho}{8\pi r_{\text{avg}}^3} \quad (30)$$

where k is the coordination number.

The number of right-hand contacts intersected by plane p is

$$\bar{Q}_r = Q_r p_r \quad (31)$$

Now consider various distribution laws for the quantity θ : Suppose θ is distributed uniformly on $[0, \pi/2]$:

$$p(\theta) = \begin{cases} 2/\pi & \in \theta [0, \pi/2] \\ 0 & \notin \theta [0, \pi/2] \end{cases}$$

$$p_r = \frac{l_{\text{avg}}}{2L} \frac{2}{\pi}$$

hence,

$$\begin{aligned}
\bar{Q}_r &= \frac{l_{\text{avg}}}{L\pi} \frac{3LS\rho k}{8\pi r_{\text{avg}}^3} \\
&= \frac{3l_{\text{avg}} S \rho k}{16\pi^2 r_{\text{avg}}^3} = \frac{3S\rho k}{8\pi^2 r_{\text{avg}}^2}
\end{aligned} \quad (32)$$

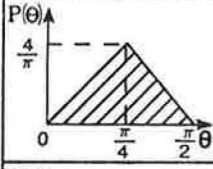
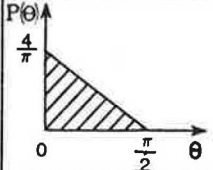
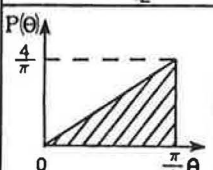
If it is assumed that, on the average, $l_{\text{avg}} = 2r_{\text{avg}}$ and that the total number of intersected contacts $Q = Q_r + Q_l = 2Q_r$,

$$Q = \frac{3\rho S k}{2\pi^2 r_{\text{avg}}^2} \quad (33)$$

Other distribution laws for θ lead to the theoretical formulas given in Table 1.

The solution obtained is in good agreement with the formula obtained by Rumpf (1)—the difference is no greater than 5 percent. A comparison of Equation 33 and the test data of Zimin and Timchenko (2) and Andriyanov and Zimon (3) showed that the difference is no greater than 12 percent, which is sufficiently accurate.

TABLE 1 THEORETICAL FORMULAS FOR DETERMINING THE NUMBER OF CONTACTS

Distribution Law for Q	Formula for Determining Number of Contacts	Transformation Coefficient to the Uniform Distribution Law
	$\bar{Q} = \frac{12kS\rho[\sqrt{2}-1]}{\pi^3 r^2}$	$n = \frac{8}{\pi}[\sqrt{2}-1] = 1.0548$
	$\bar{Q} = \frac{6 \cdot S \cdot \rho \cdot k}{\pi^3 r^2}$	$n = \frac{4}{\pi} = 1.2733$
	$\bar{Q} = \frac{6 \cdot S \cdot \rho \cdot k}{\pi^3 r^2} \left[\frac{\pi}{2} - 1 \right]$	$n = \frac{4}{\pi} \left[\frac{\pi}{2} - 1 \right] = 0.7267$

The areas of contact between particles have been determined, so it is now rather straightforward to calculate the total area of contact between the particles in a random intersecting plane and the actual contact stresses. The practical use of the theoretical solutions obtained in this paper will be discussed next.

EXAMPLES OF THE PRACTICAL USE OF THE THEORETICAL SOLUTIONS

Example 1

The contact stresses that arise on compression of a sample of asphalt concrete when the particles of the material have a uniform distribution can be calculated. The maximum and minimum radii of the spheres (which were determined by the maximum and minimum size of an individual particle) can be written in the following way with a 95 percent confidence coefficient:

$$R_1 = r_{\text{avg}}(1 + 2CV)$$

$$R_0 = r_{\text{avg}}(1 - 2CV) \quad (34)$$

The degree of interpenetration of the spheres is assumed to be $\gamma = 0.5$, and the number of contacts between particles is assumed to be 8.

The ratio of the increase in the contact stresses to the mean strength of the sample can be calculated by using

$$k_k = \frac{pS}{F_{\text{con}}p} = \frac{S}{F_{\text{con}}} \quad (35)$$

where

- p = the pressure on the sample,
- S = the area of the sample, and
- F_{con} = the area of the contacts between particles in a random cross section.

The value of F_{con} can be obtained from Equation 18 using Equation 33:

$$F_{\text{con}} = \sum_{i=1}^n \frac{2\gamma^2 \rho S k \alpha_i (R_1 - R_0)}{\pi (R_1 + R_0)^2} [3R_1 - 2\gamma(R_1 - R_0)] \quad (36)$$

where α_i is the fractional content of the i th fraction ($i = 1, 2, 3, \dots, n$). Substituting Equations 36 and 34 into Equation 35 and rearranging yields

$$k_k = \frac{\pi}{4\rho CV(3 + 2CV)} \quad (37)$$

Equation 37 was used to construct the theoretical nomogram in Figure 10. From Figure 10, it is apparent that the smaller the coefficient of variation for particle size (i.e., the closer the particles come to being spherical in shape), the higher the contact stress in the material.

Thus the strength of the sample essentially depends on the

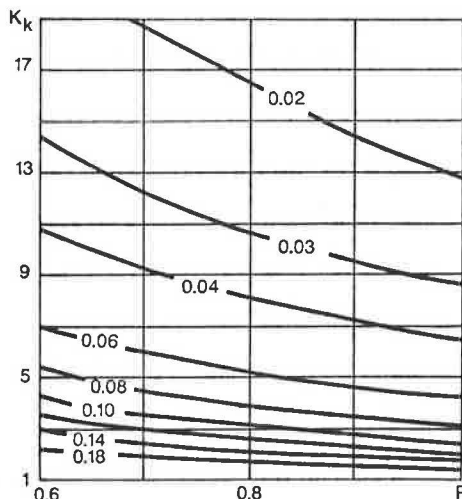


FIGURE 10 Ratio of the contact stresses and mean stresses when testing samples of material for compression, expansion, or deformation as a function of the density of the material.

shape of the particle, which is now ignored. For all practical purposes, contact stresses are inversely proportional to density.

Example 2

It is to be determined whether crushed granite will be fragmented during compaction if the particle strength is 100 MPa, the coefficient of variation of the particle sizes $CV = 0.04$, the packing load is 30 MPa, and the required density $r = 0.9$. From the nomogram in Figure 10, the permissible value of $CV = 0.07$ is obtained. Consequently, this degree of compaction can only be achieved with the material becoming fragmented.

Example 3

For the compaction of granulated material by rigid rollers (Figure 11), the exterior load is taken from the Hertz-Belyaev

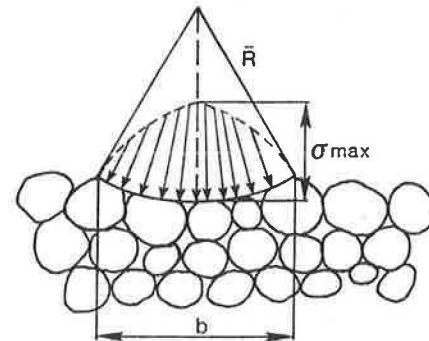


FIGURE 11 Diagram for calculating the contact stresses in the rolling of granulated (loose) materials.

solution (4) for an infinite cylinder of radius R . The maximum stress in the center of the loaded area is

$$\sigma_{\text{max}} = \frac{0.5642}{(1 - \mu^2)^{1/2}} \left(\frac{qE}{R} \right)^{1/2} \quad (38)$$

where μ and E are Poisson's coefficient and the modulus of elasticity (MPa) of the material being packed and q is the linear load per unit length of the roller (hundred weight per centimeter).

In this calculation, it is assumed that a load σ_{max} is applied to an area $d_{\text{avg}} \times d_{\text{avg}}$ (where d_{avg} is the mean size of the packed particles in centimeters). Using Equations 34–36 and 38 yields

$$k_k = \frac{12}{\pi CV(3 + 2CV)} \quad (39)$$

Equation 39 was used to construct Table 2.

Thus the shape of the crushed stone substantially affects (by a factor of as much as 12) the contact stresses directly beneath the roller. The contact stresses in the lower layers of the packed

TABLE 2 VALUE OF k_k IN THE PACKING OF MATERIAL BY RIGID ROLLERS

C_V	0.02	0.06	0.10	0.14	0.18	0.30
Value of K for k for various distributions						
U	62.82	20.40	11.94	8.32	6.32	3.54
N	78.80	25.63	15.02	10.48	7.97	4.48

Note: U = Uniform distribution and N = normal distribution.

material can be calculated using Figure 10. A comparison of the data in Table 2 and Figure 10 shows that the contact stresses in the second and subsequent layers of material are approximately a factor of 3 smaller than the stresses directly beneath the roller; this leads to fragmentation of the upper layer during rolling. To decrease the extent to which the material in the surface layer becomes fragmented, the diameter of the roller must be increased without increasing its weight, rolling should be done on a layer of elastic material (rubber, canvas, etc.), fine crushed stone or other material capable of increasing the contact area should be spread on top of the upper layer before rolling, vibrating rollers should be used, and so forth. When the sizes of the particles in the material being packed are normally distributed,

$$k_k = \frac{4}{\pi C_V \left[\frac{C_V}{2} + \left(\frac{2}{\pi} \right)^{1/2} \right]} \quad (40)$$

The theoretical results from this equation are given in Table 2. The value of k_k for the normal distribution is an average of a factor 1.255 times greater than that for the uniform distribution.

Example 4

The contact stresses for various rigid rollers will now be calculated (light rollers are less than 5 metric tons, medium rollers are 5 to 10 metric tons, and heavy rollers are 10 to 16 metric tons). A mean density $r = 0.7$ is used in the calculation. The

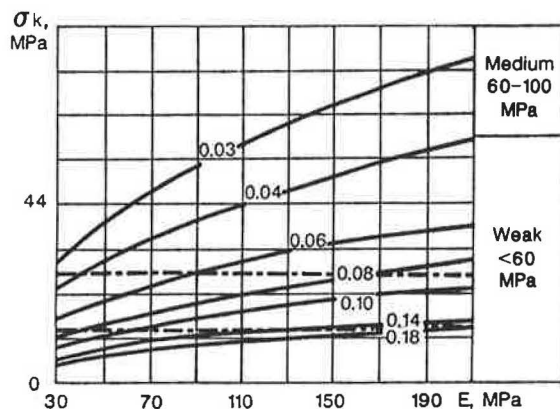


FIGURE 12 Contact stresses in crushed stone packed by a light roller.

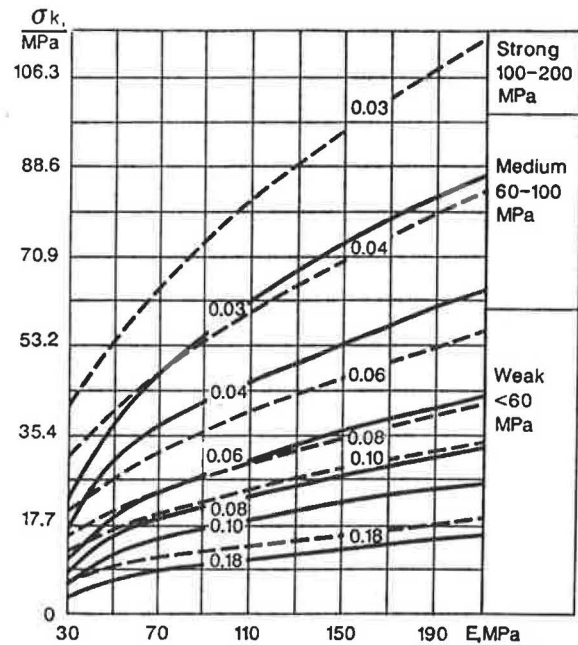


FIGURE 13 Contact stresses in crushed stone packed by a medium-weight roller.

results of the calculation are given in three nomograms (Figures 12-14), which may be used to select the roller type.

To calculate the contact stresses in the surface layer, the data in Figure 10 need to be increased by a factor of 3. The nomograms obtained (Figures 12-14) allow selection of the type of roller to be used in packing granulated materials.

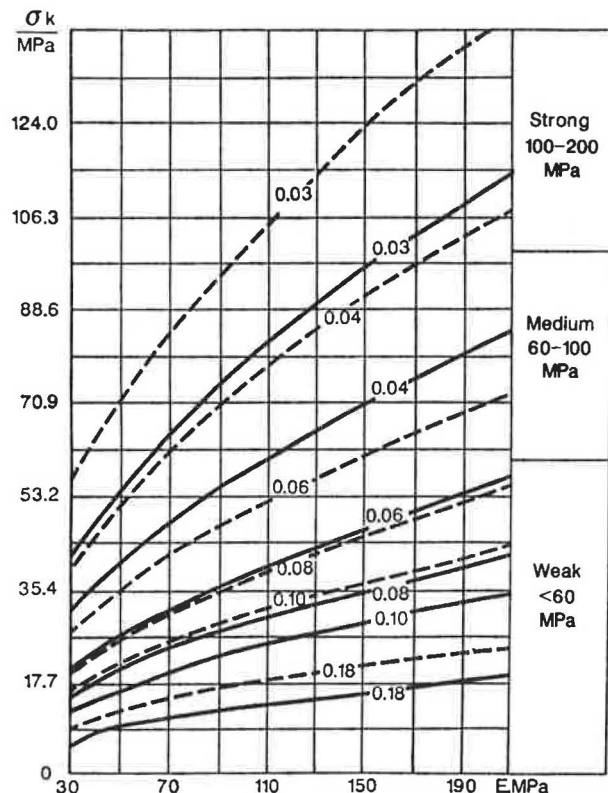


FIGURE 14 Contact stresses in crushed stone packed by a heavy roller.

Suppose that a roller must be selected to be used for packing fine limestone with a strength of 60 MPa. To avoid crushing the material, the conditions given in Table 3 must be satisfied. Thus, to preserve the particle size of the material, it must be laid on a base of less strength; the weaker the material, the weaker the base should be. The material itself should be non-uniform with respect to particle size. When the material becomes fragmented, the coefficient of variation of the particle sizes increases significantly; this leads to a sharp decrease in the contact stresses. This point is confirmed by the test data of E. A. Pospelov, obtained under the guidance of the author of this paper.

TABLE 3 SELECTION OF ROLLER TYPE

Type of Roller	Necessary Conditions for Rolling			
	For the Lower Layers of the Material Being Packed		For the Surface Layer	
	C_V	E, MPa	C_V	E, MPa
Light	≥ 0.04	≤ 210	≥ 0.08 ≥ 0.10	≤ 110 ≤ 170
Medium	≥ 0.04 ≥ 0.03	$\leq 110 - 190$ $\leq 60 - 110$	≥ 0.10 ≥ 0.08	$\leq 80 - 160$ $\leq 60 - 100$
Heavy	≥ 0.06 ≥ 0.04	$\leq 150 - 220$ $\leq 70 - 110$	≥ 0.18	≤ 170

Example 5

The packing of material by a pneumatic roller will now be discussed. When a pneumatic roller is used on packed material, the transmission of force occurs through the raised portions of the tread so that the pressure on them will be greater than the mean pressure of the wheel on the packed layer. The pressure under the raised portions of the tread for rollers in current use varies over a wide range from $q = 0.42$ to 2.4 MPa; for the most widely used rollers, $q = 0.42$ to 1.6 MPa.

Figure 10 is used for calculating the contact stresses within the layer of material being packed and Table 2 for the contact

stresses in the surface layer. Suppose that the air pressure in the roller tires is 0.6 MPa. Taking the structure of the tread into account, the pressure will be $0.6 \times 1.7 = 1.02$ MPa. The degree of packing of the material is assumed to be $r = 0.7$, and the coefficient of variation for the particle sizes $CV = 0.06$. Then the contact stresses within the layer will be $s_k = 6 \times 1.02 = 6.12$ MPa, and the stress at the surface will be $s_k = 20.4 \times 1.02 = 20.8$ MPa. If the fragmentation resistance of the material is 30 MPa, the material will not become fragmented under these packing conditions, at least not to a great extent.

CONCLUSIONS

The theoretical solution presented here allows the calculation of the engineering conditions for constructing layers with low-strength materials. Use of this method in the development of technology for packing local low-strength limestone in the Vladimir region of the USSR has made it possible to use local materials and industrial by-products widely; the usable life span of such materials in highway pavement was increased by a factor of 1.2 to 1.5, and their modulus of elasticity was increased by a factor of 1.1 to 1.3. The solution obtained can also be used to calculate the composition of the mineral mixture for asphalt concrete, cement concrete, and the like.

The theoretical solution can also be used to improve the results of laboratory tests of soils and materials.

REFERENCES

1. H. Rumpf. *Chemie-Ingenieur-Technik*, Vol. 30, No. 3, 1958, pp. 144-158.
2. M. A. Zimin and N. K. Timchenko. Standards for the Amount of Moisture in Washed Crushed Stone and Gravel to Ensure That They Do Not Freeze. In *Transactions of the All-Union Highway Scientific Research Institute* (Trudy SoyuzdorNII), No. 21, 1967, pp. 52-64.
3. A. D. Zimon and E. I. Andrianov. Autohesion of Loose Materials (Autogeziya sypuchikh materialov). *Metallurgiya*, Moscow, 1978.
4. N. M. Belyaev. Works in the Theory of Elasticity and Plasticity (Trudy po teorii uprugosti i plastichnosti), Gostekhtekhnizdat, Moscow, 1957.

Publication of this paper sponsored by Committee on Mineral Aggregates.